

RESEARCH ARTICLE

The establishment of winter wheat root system architecture in field soils: The effect of soil type on root development in a temperate climate

David J. Hobson¹  | Mary A. Harty¹ | David Langton^{2,3} | Kevin McDonnell^{1,2,3} | Saoirse R. Tracy¹

¹School of Agriculture and Food Science, University College Dublin, Belfield, Dublin 4, Ireland

²Origin Enterprises Ltd, Dublin 24, Ireland

³Biosystems Engineering Ltd, NovaUCD Belfield, Dublin 4, Ireland

Correspondence

David J. Hobson, School of Agriculture and Food Science, University College Dublin, Belfield, Dublin 4, Ireland.
Email: david.hobson@ucdconnect.ie

Funding information

Science Foundation Ireland, Grant/Award Number: 16/SPP/3296

Abstract

Winter wheat (*Triticum aestivum* L.) is an important cereal crop in the temperate climates of western Europe. Root system architecture is a significant contributor to resource capture and plant resilience. However, the impact of soil type on root system architecture (RSA) in field structured soils is yet to be fully assessed. This work studied the development of root growth using deep cultivation (250 mm) during the tillering phase stage (Zadock stage 25) of winter wheat across three soil types. The three sites of contrasting soil types covered a geographical area in the UK and Ireland in October 2018. Root samples were analysed using two methods: X-ray computed tomography (CT) which provides 3D images of the undisturbed roots in the soil, and a WinRHIZO™ scanner used to generate 2D images of washed roots and to measure further root parameters. Important negative relationships existed between soil bulk density and root properties (root length density, root volume, surface area and length) across the three sites. The results revealed that despite reduced root growth, the clay (Southoe) site had a significantly higher crop yield irrespective of root depth. The loamy sand (Harper Adams) site had significantly higher root volume, surface area and root length density compared with the other sites. However, a reduction in grain yield of 2.42 Mt ha⁻¹ was incurred compared with the clay site and 1.6 Mt ha⁻¹ compared with the clay loam site. The significantly higher rooting characteristics found in the loamy sand site were a result of the significantly lower soil bulk density compared with the other two sites. The loamy sand site had a lower soil bulk density, but no significant difference in macroporosity between sites ($p > 0.05$). This suggests that soil type and structure directly influence crop yield to greater extent than root parameters, but the interactions between both need simultaneous assessment in field sites.

This is an open access article under the terms of the [Creative Commons Attribution-NonCommercial](https://creativecommons.org/licenses/by-nc/4.0/) License, which permits use, distribution and reproduction in any medium, provided the original work is properly cited and is not used for commercial purposes.

© 2022 Origin Enterprises PLC and University College Dublin. *Soil Use and Management* published by John Wiley & Sons Ltd on behalf of British Society of Soil Science.

KEYWORDS

deep tillage, image analysis, ImageJ, root system architecture, roots, soil management, wheat, WinRHIZO™, X-ray CT

1 | INTRODUCTION

Wheat (*Triticum aestivum* L.) is an important source of human and animal nutrition globally (Shiferaw et al., 2013). However, yields have stagnated since the 1990s for many Western European countries owing to changes in climatic conditions (Brisson et al., 2010). Changing weather patterns and soil degradation driven by continuous intensive tillage resulting in organic matter loss, soil erosion and compaction threaten future crop production gains (Pagliai et al., 2004).

Root system architecture is fundamental to nutrient and water acquisition (Smith & De Smet, 2012). During the grain fill period in cereals, deep rooting can contribute significantly to final yield through water uptake. Studies based on ideotype suggest that a proliferation of fine and seminal roots with steep rooting angles capable of accessing deep soil strata would improve yields (King et al., 2003; Lynch, 2013). Moreover, Fradgley et al. (2020) discovered genotypic variation in RSA phenotypic expression of wheat under different sowing rates, growing environments and tillage regimes such as ploughing and non-inversion tillage. Selecting plant cultivars based on root resilience and plasticity will increase the success for low disturbance/alternative cultivation systems on farms (Morris et al., 2017).

Sand and clay particles have been shown to interact differently with roots under field crop management scenarios (Bacq-Labreuil et al., 2018). Coarser sandy soils when compacted become ridged, resulting in root impedance at high bulk densities (Batey, 2009). Gregorich et al. (2011) and Håkansson et al. (1988) reported greater yield penalties as penetration resistance (PR) increased under higher clay content soils. In field experiments, soil strength increases further down the soil profile because of overburden, tillage pans and compression from heavy axle loads of farm machinery (Gao et al., 2016). While root architecture studies based on sieved soil have provided important root data, it is critical to understand the effect of soil texture influences on soil structure and root growth in crop establishing field conditions (Comas et al., 2013).

X-ray CT has been successfully deployed for identifying the impacts of tillage and traffic on soil structural properties, capturing the varying differences in soil porosity and pore size distributions (Atkinson et al., 2009; Millington et al., 2017). Researchers have also applied X-ray CT to identify root traits, root responses to compaction (Tracy

et al., 2012) and for hydrology studies (Daly et al., 2015). Most root studies to date, using X-ray CT, have been confined to pot trials using sieved soil in controlled environments which offer high repeatability compared with field studies.

This paper investigated the interactions of conventional deep tillage defined as cultivation to 250 mm for this study and soil type on root system architecture across three field sites using 3D X-ray CT technology along with conventional root analysis methods to assess root and soil interactions.

2 | MATERIALS AND METHODS

2.1 | Site and soils

The trial took place during the 2018/19 growing season. The trial sites included UCD Lyons research farm, Dublin, Ireland (53.18322, -6.31398), Harper Adams University, Edmond, Newport, England (52.779738, -2.426886) and Midloe Grange farm, Southoe, Cambridgeshire, England (52.267118, -0.292297). The details of soil properties and fertility are shown in Table 1.

Three sites have a rotation of spring beans, winter wheat, winter barley (*Hordeum vulgare* L.) and oilseed rape (*Brassica napus* L.). In year two, winter wheat (*Triticum aestivum* L. cv. Graham) was drilled in all sites between September and October 2018. Harper Adams University was sown on the 5th of October (250 seeds per m²). In Lyons and Southoe, the plots were drilled (300 seeds per m²) on the 16th and 23rd of October.

2.2 | Experiment design

The experiment was conducted with one cultivation method in four replicate blocks. Each plot in Lyons was 30 m long with a 0.5 m gap between each plot, while the UK plots were 40 m long. Each plot was 3 m wide in Lyons and 4 m wide in Southoe and HAU. Tramlines were at a 90° angle to plots with 15 m spacing for fertilizing and spraying operations throughout the growing season. A split-plot design was used, half the plot (15 m) was designated for sampling and the other half was undisturbed for yield data collection. Cultivation for spring beans in Year 1 was performed at a depth of 250 mm across three sites.

TABLE 1 Soil characteristics for three trial sites

| Site | FAO | PSA | | | pH | LOI | | Average bulk density (mg m^{-3}) | | |
|--|---------------------------|----------|----------|----------|------|--------|------------|---|--------------|--|
| | | Sand (%) | Silt (%) | Clay (%) | | OM (%) | 0–100 (mm) | 100–200 (mm) | 200–300 (mm) | |
| Lyons Farm, University College Dublin | Calcaric groundwater gley | 33.24 | 39.23 | 27.64 | 6.5 | 6.72 | 1.34 | 1.39 | 1.46 | |
| Grange farm, Southoe, Cambridgeshire | Calcaric stagnic cambisol | 26 | 29 | 45 | 7.93 | 3 | 1.29 | 1.42 | 1.56 | |
| Large Marsh, Harper Adams University (HAU) | Claverley*/Regosol | 74.5 | 11.15 | 14.35 | 6.3 | 4.51 | 1.35 | 1.46 | 1.56 | |

Abbreviations: FAO class, Food and Agricultural Organisation* (Beard, 1988); LOI, Loss on ignition; OM, Organic matter; PSA, Particle size analysis.

In Lyons, HAU and Southoe, cultivation took place using a chisel plough consisting of tines. A Horsch® joker with ‘TerraGrip tines’ (600 mm spacing) was used in Lyons to 250 mm. In HAU, a Vaderstad® Topdown was used with tines cultivation to 250 mm depths. In Southoe, a Lemken® Karat 9 was used to the same depth.

2.3 | In field agronomy and yield measurement

In UCD Lyons, a base compound of N, Phosphorus (P), Potassium (K) and Sulphur (S) (10–5–25+Sulphur) was applied at early stem extension (GS30) in March. The main split of N was applied as urea (46% N) at GS32 (160 kg/N/ha) followed by the final application at GS37 (54 kg/N/ha) in June using CAN (27% N) (calcium ammonium nitrate). A pre-emergent herbicide was applied. Fungicide applications were at GS 32, 39 and 61 to protect important yield forming leaves and grain ears. Straw was chopped at all three sites after harvest. UK sites were fertilized in accordance with the AHDB guidelines and soil fertility test analysis (AHDB, 2018). A plot combine was used for each site with total plot yields (t ha^{-1}) calculated from the weight of the grain collected by the combined load cells. Moisture was adjusted to 15% for yield calculations.

2.4 | Soil core sampling and soil physical parameters

The root core size was chosen to capture as much root material growing in the field as possible while minimizing the trade-off that exists with the X-ray CT technology between image resolution and core size. One soil core was extracted from each plot at growth stage (GS) 25 tillering ca. 15 weeks after sowing. Polyvinyl chloride (PVC) drainage pipes were cut to size (70 × 300 mm) and these tubes were used to collect soil cores. Tubes with a diameter of 70 mm were inserted to 300 mm into the soil in the crop rows between the wheel tracks using a mallet to ensure that root samples were not affected by wheel induced soil compaction. A single wheat plant sample was located at random in each plot. The selected plant was cut at the base of the stem and above-ground biomass was discarded. The PVC tube was placed over the remaining plant stubble (centred) to maximize root system capture. Following sampling, cores were sealed (top and bottom) using tape and labelled. The soil core was extracted carefully using a spade and sample locations were backfilled. Cores were tightly packed to minimize movement during transit of samples to the laboratory for analysis. Samples were stored at 4°C.

Soil bulk density core samples using an Eijkelkamp® soil corer were collected from each plot in the non-trafficked area. Samples were replicated three times. Each core sample was 50 mm in diameter and 300 mm in length. Each bulk density sample was taken within 0.5 m of the location of the soil cores taken for X-ray CT. Intact fresh soil cores were weighed prior to drying and sample fresh weights were recorded. Samples were placed into an oven at 105°C for 24 h and reweighed to determine moisture % and dry bulk density (Campbell & Henshall, 2001).

2.5 | X-ray computed tomography (CT)

The soil cores were scanned using a Phoenix® v|tome|x M 240 kV scanner at UCD (GE Measurement and Control solution, Wunstorf, Germany). The v|tome|x M was set at a voltage of 90 kV and a current of 400 µA to optimize contrast between background soil and root material. A voxel resolution of 45 µm was achieved by using the 'Multi Scan option' to scan in 4 segments. A total of 1800 projection images were taken per scan at 200 m/s per image. Once scanning was complete, the images were reconstructed using Phoenix datos|x2 rec reconstruction software, the four scans were assembled into one 3D volume for the whole core.

2.6 | Destructive 2D root analysis

After the soil cores were X-ray CT scanned the soil and root material were separated by root washing. Three sets of sieves with a mesh size of 2, 1 and 0.5 mm were used to collect root material. The washed root samples were placed into a freezer until scanning and analysis with WinRHIZO™ scanning and software commenced. Root images were scanned at a resolution of 600 dpi (945 pixels) for root length, root surface area, average root diameter and root volume for the total soil core. Root length is calculated by the number of pixels in the root skeleton multiplied by the pixel size. The WinRHIZO™ estimates the average diameter from the total projected root area and length. The formula and calculations for each root parameter are based on the methods described in Regent Instruments (2016). The WinRHIZO™ calculated the root volume by determining the average root diameter and root length by pixel counting the 2D root image. The output of the images was distinguished by global thresholding analyses for root diameter while root length was validated by skeleton images. After WinRHIZO™ scanning, the root samples were dried at 70°C for 24 h and the root biomass samples were weighed.

2.7 | X-ray CT root segmentation

Image analysis for X-ray CT images was performed using the software VGStudioMax® version 3.2 (Volume Graphics GmbH, Heidelberg, Germany) to segment roots and analyse soil porosity. Roots were segmented by setting seed points and using selected threshold values in *Region grower* enabling selection of grey-scale pixels pertaining to root materials. The root system was traced from the starting point selected at the top of the root system and followed down through the sliced images. Once the roots were segmented from the image, erosion and dilation tool was selected at 1 pixel using the *Region Growing* tool. Root system architecture parameters such as root length, root volume and root surface area were measured from the segmented root systems.

2.8 | Soil porosity analysis

Before analysis on ImageJ 1.52 (Schneider et al., 2012) software could commence, an image stack was created in VG Studio Max® for each scan. Scan volumes were cropped as a cylinder and the tube edges and air space outside of the soil core were removed. The *surface determination tool* in VG Studio Max® was used to threshold pore spaces within the solid matrix. The tool defines the contour of objects, separating 3D data into regions. The image was then inverted to remove the extracted variables from the image and highlight the pore spaces in the soil core.

The ImageJ Huang automatic threshold algorithms were used for each scan to separate the pores from the solid matrix. The binarized scans were de-speckled twice to remove unwanted noise within each scanned image, improving the analysis and accuracy of the investigated pores. The resulting binary images were analysed using the Analyze Particles tool which provided information for average pore size, total area and percentage porosity for each individual image.

2.9 | Soil moisture deficit model

Soil moisture deficit (SMD) was calculated based on the SMD hybrid model for Irish grassland (Schulte et al., 2005). It is a water mass balance model with daily measurements in minimum and maximum temperature, rainfall (mm), wind speed at 10 metres height (m/s) and sunshine hours. These measurements enable the calculation of evapotranspiration and radiation. This model predicts soil moisture deficit based on three soil drainage classifications for well drained sandy loam soils, medium drained loam soils and

poorly drained gley soils and local weather conditions taken from the nearest weather station.

2.10 | Statistics

Data from the scanned (destructive and non-destructive) images and root biomass were not normally distributed, therefore all data were log-transformed (in Microsoft Excel) before being exported to Minitab 18[®] where analysis of variance (ANOVA) was performed. ANOVA (Minitab 18[®]) was conducted and the differences between means were determined using the Tukey post hoc test at the 95% confidence level.

3 | RESULTS

3.1 | Growing conditions during crop season

For the winter cropping year (October–August), rainfall was higher in Lyons (738.9 mm) compared with a 30-year average of 612.3 mm (Met Eireann, 2020). Rainfall

levels varied between sites with considerably more rainfall in Lyons than in HAU and Southoe. From January to August, 418.6 mm of rainfall was recorded at HAU (68 mm total for January and February). In the same period, 316.2 mm fell in Southoe and 489.6 mm in Lyons. Soil moisture deficit values (Figure 1) for Lyons reached 40.5 mm at the start of June. The soil moisture deficits were 87.83 mm in Southoe and 66.2 mm in HAU by May and early June, respectively. In contrast, high rainfall levels in August (113 mm), meant harvest occurred at field capacity in Lyons.

3.2 | Root measurements

The destructive scans showed that HAU had significantly higher root volume ($p < 0.05$), root surface area ($p < 0.01$), root length density ($p < 0.001$) and root length ($p < 0.001$) than both Lyons and Southoe (Table 2). Root length at HAU was over two-fold greater than at Lyons and Southoe (HAU = 7869 mm, Lyons = 3078 mm, Southoe = 3819 mm). In contrast, the Lyons site had a significantly greater root diameter (0.335 mm) than the other sites (Southoe = 0.300 mm, HAU = 0.272) ($p < 0.001$).

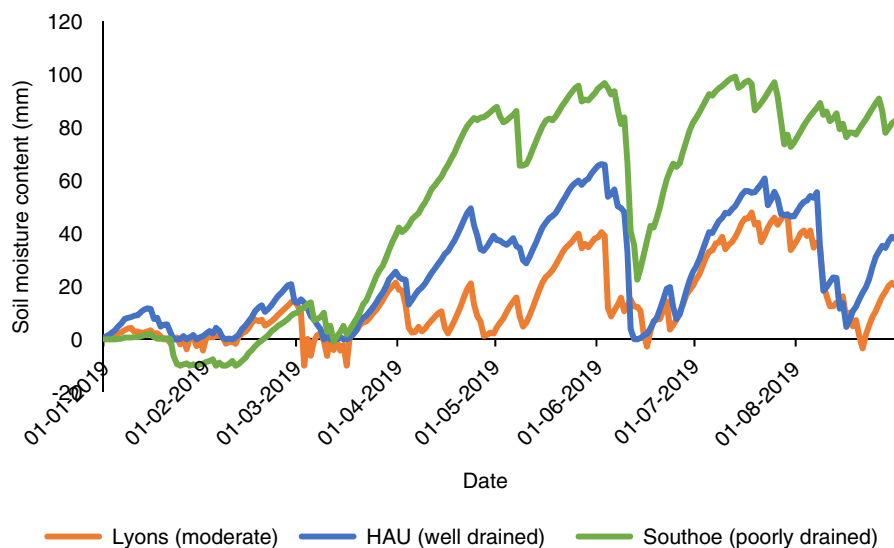


FIGURE 1 Soil moisture deficit (SMD) in moderately drained (Lyons), well-drained (HAU) and poorly drained soil (Southoe) from January to August 2019. High SMD in May and June during key leaf forming growth stages (GS32–39) may have caused early senescence in well drained sites

TABLE 2 Root system architecture parameters calculated using destructive root method

| Site | WinRHIZO results | | | | |
|----------------|--------------------------------|---------------------------------|--------------------|--|------------------|
| | Root volume (mm ³) | Surface area (mm ²) | Root diameter (mm) | Root length density (mm/m ³) | Root length (mm) |
| Lyons | 268b | 3213b | 0.3354a | 2667b | 3078b |
| Southoe | 269b | 3590b | 0.3007b | 3309b | 3819b |
| HAU | 456a | 6714a | 0.2724c | 6818a | 7869a |
| <i>p</i> value | 0.013 | 0.003 | 0.001 | 0.001 | 0.001 |

*Significant differences between means are represented by different letters.

Southoe root diameter was significantly greater than HAU and significantly smaller than Lyons ($p < 0.001$).

HAU had a slightly higher mean root biomass 0.048 g. Lyons and Southoe had root biomass of 0.043 and 0.020 g, respectively (Figure 2). Although the root biomass differences were not significant, the trends in root biomass results were higher for HAU than Lyons and Southoe which followed similar trends found in destructive and non-destructive root analysis results.

There was a significantly greater root surface area (6714 mm²) for wheat roots at HAU ($p < 0.01$) compared with Southoe and Lyons (Table 3). Root volume was also higher in HAU (363.5 mm³) compared with Southoe and

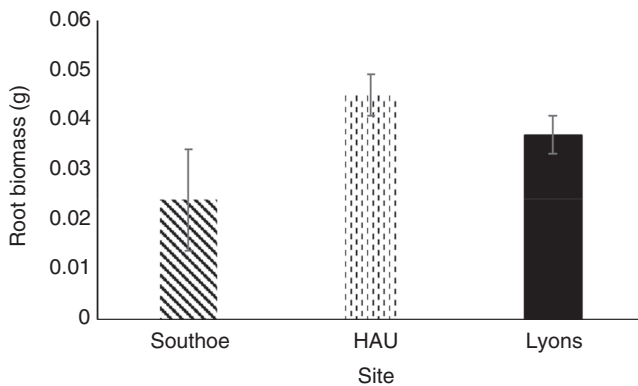


FIGURE 2 Root biomass (g) × site

Lyons (200 and 181.5 mm³ respectively) though the differences were not significant. Vertical root depth, root length density and root volume did not significantly differ between sites (measured via the z-axis on VGStudioMax[®]). Similarly, root width showed no difference between the three sites.

3.3 | Soil properties and root response to bulk density

Deep tillage had different effects on soil physical conditions across three sites (Table 4). In the top 100 mm, soil bulk density was significantly lower in HAU than in Lyons and Southoe ($p < 0.05$). In the middle soil horizon between 100 and 200 mm, a significant interaction between site and tillage was found. Bulk density was significantly lower in HAU compared with Southoe ($p < 0.05$). In the bottom 200–300 mm layer measured, no tillage interaction with site difference was found ($p > 0.05$).

3.4 | Soil macroporosity

In the top and middle sections (0–100 mm, 100–200 mm respectively), no significant difference was found between the sites (Figure 3). Significant differences

TABLE 3 Root system architecture parameters calculated using non-destructive method

| Site × tillage | 3D root architecture | | | | |
|----------------|----------------------|--------------------------------|---------------------------------|---|-------------------------|
| | η | Root volume mm ³ | Surface area mm ² | Root length density (mm/m ³) | Length (Z) axis (mm) |
| Lyons | 4 | 181.1a | 1402b | 40.67a | 46.93a |
| Southoe | 4 | 200a | 1332b | 45.4a | 54.4a |
| HAU | 3 | 363.5a | 2290.9a | 70.3a | 81.2a |
| <i>p</i> value | | 0.149 | 0.008 | 0.335 | 0.335 |

*Significant differences between means are represented by different letters.

TABLE 4 Soil bulk density for deep tillage x site interaction for three depth layers analysed

| Site × tillage | η | Bulk density (t m ⁻³) 0-300mm depth | | | | | |
|----------------|--------|--|------------|---------------------|------------|---------------------|------------|
| | | 0-100 mm Means | SEM (±) | 100-200 mm Means | SEM (±) | 200-300 mm Means | SEM (±) |
| Lyons | 3 | 1.28ab | 0.023 | 1.23ab | 0.047 | 1.52a | 0.046 |
| Southoe | 3 | 1.31b | 0.07 | 1.33 b | 0.099 | 1.507a | 0.098 |
| HAU | 3 | 1.044a | 0.077 | 1.105a | 0.103 | 1.425a | 0.107 |
| <i>P</i> value | | 0.044 | | 0.042 | | 0.691 | |

*Significant differences between means are represented by different letters.

between sites ($p < 0.01$) were observed in the lower soil layer (200–300 mm). Southoe had significantly lower macroporosity than HAU and Lyons. The total pore surface area showed no significant difference across the three soil layers.

3.5 | Crop yield

The interaction between grain yield and site was highly significant ($p < 0.001$) (Figure 4). HAU produced the lowest yield (10.89 t/ha) and had increased rooting compared with Southoe and Lyons (13.31 and 12.49 t/ha respectively).

4 | DISCUSSION

4.1 | Soil type, weather and crop yield

Grain yield was significantly affected by soil type in this experiment, the increased fertility and water holding capacity of higher clay soils and organic matter contents in Southoe and Lyons improved grain yield compared with the sandy texture and low organic matter at HAU. The highest soil moisture deficit for Lyons was recorded in the middle of July at 47.8 mm but it is unlikely that moisture stress impacted crop yield at Lyons. HAU received a total rainfall of 232.3 mm from November 2018 to May 2019. HAU was in a soil moisture deficit for 230 days (Figure 1) with a deficit of 65.9 mm in June; coupled with lower organic matter levels and poor moisture retentive soil, it is likely to have limited yield during critical leaf forming growth stages. Lyons which was in a modest SMD for 221 days had lower moisture deficits in June (8.68 mm), higher clay content and organic matter which may have reduced the yield impact. Southoe recorded the highest soil moisture daily deficits and had the fewest number of days in deficit (196 days). The high moisture retentive properties of the Southoe *Hanslope* soil series may have prevented plants from suffering moisture stress.

4.2 | Soil bulk density and root growth

In the HAU site rooting depth was confined to the top 100 mm of soil at the time of sampling. HAU is a long-term controlled traffic tillage site for 8 years and had the lowest bulk density. Soil types responded differently to cultivation with increased root growth during crop establishment and tillering in HAU. However, Lyons and Southoe yielded significantly higher than HAU, and Southoe and Lyons had significantly less root growth than HAU. This may be an indication that plants developed greater aboveground biomass (not measured) under less stress as the smaller roots in these sites did not appear to have an impact on yield. At HAU, a lack of moisture reduced above-ground biomass in response to stress.

HAU had the lowest bulk density (1.044 t m^{-3}) in the top 100 mm showing the least impedance to root growth compared with 1.3 to 1.5 t m^{-3} for the HAU site (Czyż, 2004; Hamza & Anderson, 2005). However, this would likely cause moisture and nutrient retention issues during drier periods of the growing season (Alameda et al., 2012). The bulk density in Lyons (1.28 t m^{-3}) was closer to the ideal bulk density of $1.54\text{--}1.58 \text{ t m}^{-3}$ reported by Czyż (2004) for loamy soils. Lower bulk density would support the significant increase in root development in HAU as HAU had longer time to recover from random traffic farming and previous soil management practices which were experienced at the shorter-term Lyons and Southoe trial sites.

4.3 | Soil macroporosity

Although significant differences in bulk density were found between sites, the differences in macroporosity and pore size were less pronounced (Figure 3). In clay soils, it is suggested that plant roots increase soil porosity through greater pore size heterogeneity (Bacq-Labreuil et al., 2018). An increase in bulk density in HAU would have significantly reduced porosity and root growth compared with the other two sites because of less aggregation

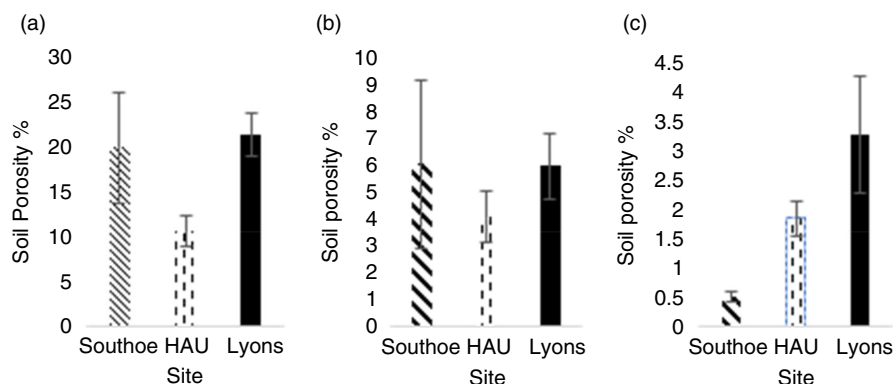


FIGURE 3 Total soil porosity calculated from CT for Southoe, HAU and Lyons for three soil layers (a) 0–100 mm, (b) 100–200 mm & (c) 200–300 mm

and higher friction between coarse particles (Batey, 2009). Southoe had significantly ($p < 0.01$) lower subsoil macroporosity (0.51%) than HAU and Lyons, all sites indicated poor aerobic subsoil conditions for root growth with only 1.84% macro-porosity at HAU and 3.28% in Lyons. This low level of macroporosity is inversely related to the high bulk densities found at the 200–300 mm soil section. Deep tillage did not improve the 200–300 mm soil environment across the three sites as seen in vertical view using X-ray CT (Figure 5). Compacted anaerobic conditions would adversely affect root elongation and resource capture during

the latter growth stages of the crop (Mosaddeghi et al., 2009). In the top 0–100 mm as well as the 100–200 mm layer, Southoe had significantly higher bulk density than HAU but not significantly different to Lyons. The X-ray CT scans showed shorter, thicker root growth in both sites compared with HAU (Figure 6). The higher soil bulk density levels found in Lyons increased root diameter significantly compared with HAU ($p < 0.001$) which is a response reported by Tracy et al. (2012). HAU had a significantly lower root diameter than Southoe and Lyons. Southoe had a significantly lower root diameter than Lyons but significantly higher than HAU.

This study shows through X-ray CT that soil porosity did not improve in the lower soil sections analysed. Soil type may be a possible reason for high bulk density and low porosity in Southoe, with high silt levels in the subsoil causing collapsing of natural soil structure and compaction from cultivation instead of loosening (Schneider et al., 2017). Southoe had the highest bulk density (1.31 t m^{-3}) yet had greater macroporosity than HAU and Lyons in the upper soil layers and significantly less porous in subsoil layers (Figure 5). The high clay content (45%) would support higher porosity. This study suggests that the clay % of soil was more important for crop yield when smaller root systems are present, compared with rooting depth.

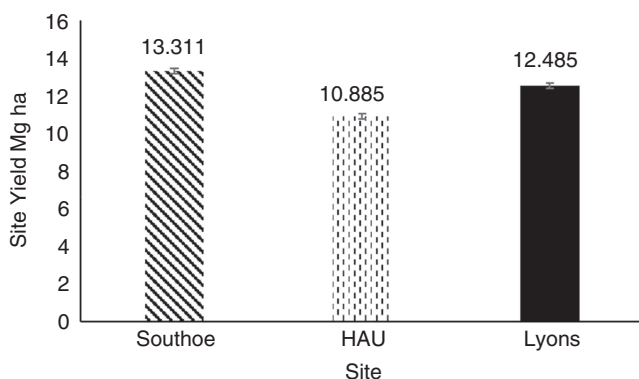


FIGURE 4 The mean yield of winter wheat cv. Graham across three sites

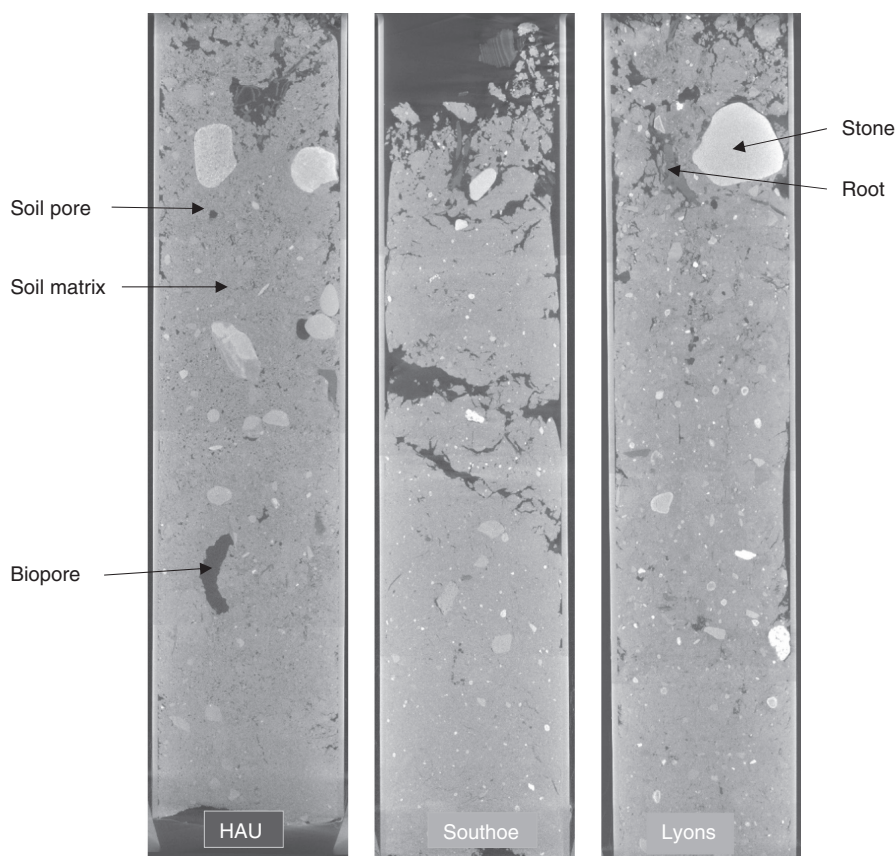


FIGURE 5 Vertical view of X-ray CT images through the centre of soil cores produced using VGStudioMax® software on three field sites. Scale bar at the base of images is 50 mm

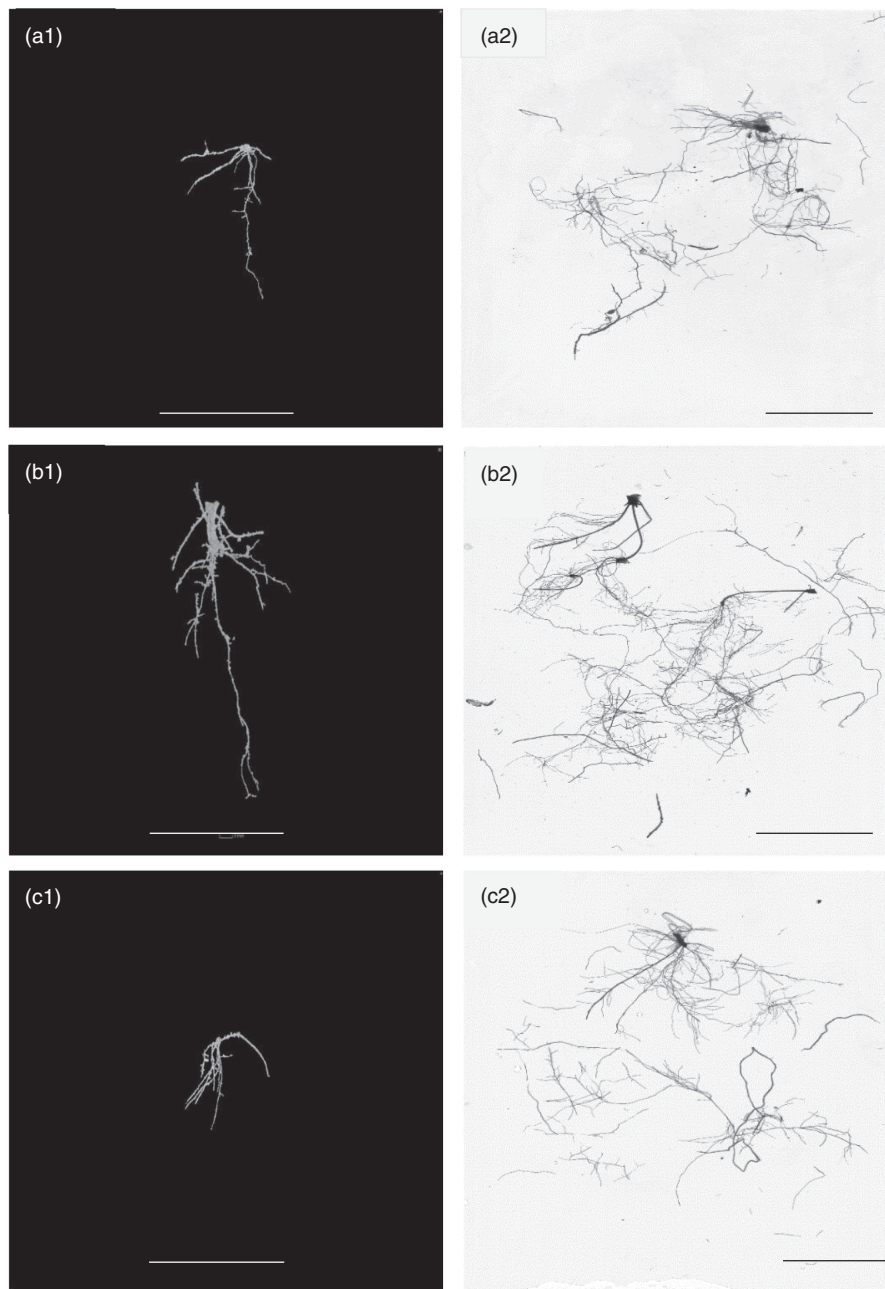


FIGURE 6 A1, B1 and C1 are the RSA of wheat at Lyons, HAU and Southoe, respectively. A2, B2, C2 are the corresponding root system scanned with the WinRHIZO™ scanner, respectively. C1 shows a typical RSA found in Southoe under high bulk density, leading to reduced vertical rooting and increased horizontal spread. Scale bar A1, B1 and C1 = 70 mm. Scale bar A2, B2 and C2 = 50 mm

4.4 | Root parameters

Figure 6 illustrates typical root images post root washing and analysis for both non-destructive and destructive methods. Higher bulk density and lower soil porosities found in Southoe and Lyons were reflected in rooting properties important for moisture retention. The decreased surface area and root volume compared with the HAU root system did not translate to negative impacts on crop yield on Southoe. HAU showed the greatest seminal root depth and RLD of 80.1 mm and 70.1 mm respectively at the tillering growth stage, detected by the non-destructive method at 45 μm .

Other studies reported a lack of throughput by X-ray CT methods for quantitative field studies (Zhu et al., 2011). This study supports previously published work by Tracy et al. (2012), Zappala et al. (2013) and Valentine et al., (2012), proving that modern “fast scanning” technologies demonstrate the ability for X-ray CT to produce medium throughput for large, replicated field trial studies. Image analysis uncovered the vertical root depth (Z-axis) for each segmented scan, highlighting the rooting patterns of seminal roots in response to tillage (Figure 6). The destructive method proved a useful method for highlighting root response to bulk density. No relationship was found between bulk density and X-ray CT images which

represent the main root axes and some lateral rooting. However, unlike WinRHIZO™, finer roots could not be segmented as a higher resolution and a smaller core size would be required.

5 | CONCLUSIONS

The results of this study indicate that soil type has a significantly greater influence on crop yield than total root growth. The yield was greatest on the high clay site (13.33 t ha⁻¹) compared with HAU on the sandy loam site (10.9 t ha⁻¹) suggesting that root exploration differed between soil types and their ability to acquire resources. The clay site increased grain yield (0.450 t ha⁻¹) under similar management by 2.42 t ha⁻¹ compared with the sandy loam site at HAU (0.143 t ha⁻¹). X-ray CT has shown value for obtaining data on root and soil properties on large replicated field trials.

ACKNOWLEDGEMENT

We acknowledge the financial contribution of Origin Enterprises and Science Foundation Ireland, Grant number: 16/SPP/3296. Open access funding provided by IREL. [Correction added on 19 May 2022, after first online publication: Projekt CRUI-CARE funding statement has been added.]

ORCID

David J. Hobson  <https://orcid.org/0000-0001-8136-7434>

REFERENCES

- AHDB (2018). *Wheat growth guide*, AHDB Cereals & Oilseeds, Stoneleigh Park, Kenilworth, Warwickshire, CV8 2TL: AHDB.
- Alameda, D., Anten, N. P. R., & Villar, R. (2012). Soil compaction effects on growth and root traits of tobacco depend on light, water regime and mechanical stress. *Soil and Tillage Research*, 120, 121–129. <https://doi.org/10.1016/j.still.2011.11.013>
- Atkinson, B. S., Sparkes, D. L., & Mooney, S. J. (2009). Effect of seed-bed cultivation and soil macrostructure on the establishment of winter wheat (*Triticum aestivum*). *Soil and Tillage Research*, 103(2), 291–301. <https://doi.org/10.1016/j.still.2008.10.027>
- Bacq-Labreuil, A., Crawford, J., Mooney, S. J., Neal, A. L., Akkari, E., McAuliffe, C., Zhang, X., Redmile-Gordon, M., & Ritz, K. (2018). Effects of cropping systems upon the three-dimensional architecture of soil systems are modulated by texture. *Geoderma*, 332, 73–83. <https://doi.org/10.1016/j.geoderma.2018.07.002>
- Batey, T. (2009). Soil compaction and soil management – a review. *Soil Use and Management*, 25(4), 335–345.
- Beard, G. R. (1988). *The soils of Harper Adams Agricultural College*. Shropshire, Newport, Silsoe: Published by Soil Survey and Land Research Centre.
- Brisson, N., Gate, P., Gouache, D., Charmet, G., Oury, F.-X., & Huard, F. (2010). Why are wheat yields stagnating in Europe? A comprehensive data analysis for France. *Field Crops Research*, 119(1), 201–212. <https://doi.org/10.1016/j.fcr.2010.07.012>
- Campbell, D. J., & Henshall, J. K. (2001). Bulk density. In K. A. Smith, & C. E. Mullins (Eds.), *Soil and Environment Analysis : Physical Methods* (pp. 315–348). New York: American Society of Agronomy.
- Comas, L. et al. (2013). Root traits contributing to plant productivity under drought. *Frontiers in Plant Science*, 4, 442.
- Czyż, E. A. (2004). Effects of traffic on soil aeration, bulk density and growth of spring barley. *Soil and Tillage Research*, 79(2), 153–166. <https://doi.org/10.1016/j.still.2004.07.004>
- Daly, K. R., Mooney, S. J., Bennett, M. J., Crout, N. M. J., Roose, T., & Tracy, S. R. (2015). Assessing the influence of the rhizosphere on soil hydraulic properties using X-ray computed tomography and numerical modelling. *Journal of Experimental Botany*, 66(8), 2305–2314. <https://doi.org/10.1093/jxb/eru509>
- Eireann, M. (2020). *Monthly Data - Casement Aerodrome*. Available at: <https://Met.ie/climate/available-data/monthly-data>. Accessed on 4 Feb 2020.
- Fradgley, N., Evans, G., Biernaskie, J. M., Cockram, J., Marr, E. C., Oliver, A. G., Ober, E., & Jones, H. (2020). Effects of breeding history and crop management on the root architecture of wheat. *Plant and Soil*, 452(1), 587–600. <https://doi.org/10.1007/s11104-020-04585-2>
- Gao, W., Hodgkinson, L., Jin, K., Watts, C. W., Ashton, R. W., Shen, J., Ren, T., Dodd, I. C., Binley, A., Phillips, A. L., Hedden, P., Hawkesford, M. J., & Whalley, W. R. (2016). Deep roots and soil structure. *Plant, Cell & Environment*, 39(8), 1662–1668. <https://doi.org/10.1111/pce.12684>
- Gregorich, E. G., Lapen, D. R., Ma, B. L., McLaughlin, N. B., & VandenBygaart, A. J. (2011). Soil and crop response to varying levels of compaction, nitrogen fertilization, and clay content. *Soil Science Society of America Journal*, 75(4), 1483–1492. <https://doi.org/10.2136/sssaj2010.0395>
- Håkansson, I., Voorhees, W. B., & Riley, H. (1988). Vehicle and wheel factors influencing soil compaction and crop response in different traffic regimes. *Soil and Tillage Research*, 11(3), 239–282. [https://doi.org/10.1016/0167-1987\(88\)90003-7](https://doi.org/10.1016/0167-1987(88)90003-7)
- Hamza, M. A., & Anderson, W. K. (2005). Soil compaction in cropping systems: A review of the nature, causes and possible solutions. *Soil and Tillage Research*, 82(2), 121–145. <https://doi.org/10.1016/j.still.2004.08.009>
- King, J. et al. (2003). Modelling cereal root systems for water and nitrogen capture: towards an economic optimum. *Annals of Botany*, 91(3), 383–390. <https://doi.org/10.1093/aob/mcg033>
- Lynch, J. P. (2013). Steep, cheap and deep: an ideotype to optimize water and N acquisition by maize root systems. *Annals of Botany*, 112(2), 347–357. <https://doi.org/10.1093/aob/mcs293>
- Millington, W. A. et al. (2017). *An investigation into the effect of traffic and tillage on soil properties using X-ray computed tomography*. 2017 ASABE Annual International Meeting, pp. 1.
- Morris, E. C., Griffiths, M., Golebiowska, A., Mairhofer, S., Burr-Hersey, J., Goh, T., Wangenheim, D., Atkinson, C. J., Sturrock, A., Lynch, J. P., Vissenberg, K., Ritz, K., Wells, D. M., Mooney, S. J., & Bennett, M. J. (2017). Shaping 3D system architecture. *Current Biology*, 27(11), 919–930.
- Mosaddeghi, M. R., Mahboubi, A. A., & Safadoust, A. (2009). Short-term effects of tillage and manure on some soil physical properties and maize root growth in a sandy loam soil in western

- Iran. *Soil and Tillage Research*, 104(1), 173–179. <https://doi.org/10.1016/j.still.2008.10.011>
- Pagliai, M., Vignozzi, N., & Pellegrini, S. (2004). Soil structure and the effect of management practices. *Soil and Tillage Research*, 79(2), 131–143. <https://doi.org/10.1016/j.still.2004.07.002>
- Regent Instruments (2016). *WinRHIZO*. Regent instruments Inc, University of Quebec, Canada
- Schneider, C. A., Rasband, W. S., & Eliceiri, K. W. (2012). NIH Image to ImageJ: 25 years of image analysis. *Nature Methods*, 9(7), 671–675. <https://doi.org/10.1038/nmeth.2089>
- Schneider, F. et al. (2017). The effect of deep tillage on crop yield – What do we really know? *Soil and Tillage Research*, 174, 193–204. <https://doi.org/10.1016/j.still.2017.07.005>
- Schulte, R. P. O., Diamond, J., Finkle, K., Holden, N. M., & Brereton, A. J. (2005). Predicting the soil moisture conditions of Irish Grasslands. *Irish Journal of Agricultural and Food Research*, 44(1), 95–110.
- Shiferaw, B., Smale, M., Braun, H.-J., Duveiller, E., Reynolds, M., & Muricho, G. (2013). Crops that feed the world 10. Past successes and future challenges to the role played by wheat in global food security. *Food Security*, 5(3), 291–317. <https://doi.org/10.1007/s12571-013-0263-y>
- Smith, S., & De Smet, I. (2012). Root system architecture: insights from Arabidopsis and cereal crops. *Philosophical Transactions of the Royal Society B: Biological Sciences*, 367(1595), 1441–1452.
- Tracy, S. R., Black, C. R., Roberts, J. A., McNeill, A., Davidson, R., Tester, M., Samec, M., Korošak, D., Sturrock, C., & Mooney, S. J. (2012). Quantifying the effect of soil compaction on three varieties of wheat (*Triticum aestivum* L.) using X-ray micro computed tomography (CT). *Plant and Soil*, 353(1), 195–208. <https://doi.org/10.1007/s11104-011-1022-5>
- Valentine, T. A., Hallett, P. D., Binnie, K., Young, M. W., Squire, G. R., Hawes, C., & Bengough, A. G. (2012). Soil strength and macropore volume limit root elongation rates in many UK agricultural soils. *Annals of Botany*, 110(2), 259–270. <https://doi.org/10.1093/aob/mcs118>
- Zappala, S., Mairhofer, S., Tracy, S., Sturrock, C. J., Bennett, M., Pridmore, T., & Mooney, S. J. (2013). Quantifying the effect of soil moisture content on segmenting root system architecture in X-ray computed tomography images. *Plant and Soil*, 370(1), 35–45. <https://doi.org/10.1007/s11104-013-1596-1>
- Zhu, J., Ingram, P. A., Benfey, P. N., & Elich, T. (2011). From lab to field, new approaches to phenotyping root system architecture. *Current Opinion in Plant Biology*, 14(3), 310–317. <https://doi.org/10.1016/j.pbi.2011.03.020>

How to cite this article: Hobson, D. J., Harty, M. A., Langton, D., McDonnell, K., & Tracy, S. R. (2023). The establishment of winter wheat root system architecture in field soils: The effect of soil type on root development in a temperate climate. *Soil Use and Management*, 39, 198–208. <https://doi.org/10.1111/sum.12795>